Bilayer-Structured Regenerated Cellulose/Chitosan Films Prepared with Ionic Liquid

Faisal Amri Tanjung[1,*], Yalun Arifin[1,2], Abdul Hamid Abdullah[3], and Iqmal Tahir[4]

[1]*Department of Chemical Engineering, Faculty of Engineering and Sciences, Curtin University Sarawak, CDT 250, 98009 Miri, Sarawak, Malaysia*

[2]*Department of Food Business Technology, Prasetya Mulya University, BSD Raya Utama, Kabupaten Tangerang 15339, Indonesia*

[3]*Department of Petroleum Engineering, Faculty of Engineering and Sciences, Curtin University Sarawak, CDT 250, 98009 Miri, Sarawak, Malaysia*

[4]*Department of Chemistry, Faculty of Mathematics and Natural Sciences, Universitas Gadjah Mada, Sekip Utara, Yogyakarta 55281, Indonesia*

Received April 25, 2017; Accepted September 8, 2017

ABSTRACT

The effects of chitosan on properties of regenerated cellulose/chitosan (RC/Ch) films were investigated. The films were prepared using a sequence process of solution-casting in a lithium chloride/N,N-dimethylacetamide ionic liquid, and coagulation in water. Due to the amorphous structure of chitosan and the formation of hydrogen bonding between the functional groups of the both components, tensile strength of the films decreased considerably; however, elongation at break increased. Furthermore, SEM morphology indicated a visible separated layers comprising of rigid and ductile surfaces. The addition of chitosan clearly improved the thermal stability of the films, although the thermal degradation mechanism was not altered.

Keywords: *cellulose; chitosan; laminate; mechanical properties; thermal properties; thin film*

ABSTRAK

Pengaruh khitosan pada sifat-sifat lapisan selulosa/khitosan teregenerasi telah dikaji. Lapisan tersebut dibuat dengan sederetan proses meliputi penuangan larutan selulosa/khitosan pada cairan ionik lithium khlorida/N,N-dimetilasetamida dan proses koagulasi di dalam air. Mengingat struktur amorf dari khitosan dan pembentukan ikatan hidrogen di antara gugus-gugus fungsional pada kedua kedua bahan, maka kekuatan tensil dari film diduga akan berkurang, namun elongasi pemutusan akan meningkat. Gambaran morfologi SEM mengindikasikan lapisan-lapisan yang tampak terpisah dengan gambaran permukaan yang kompak dan ulet. Penambahan khitosan secara nyata meningkatkan kestabilan termal lapisan, meskipun mekanisme degradasi termal tidak berubah.

Kata Kunci: *khitosan; laminasi; lapis tipis; selulose; sifat mekanik; sifat termal*

INTRODUCTION

New bio-based composite materials that are renewable and biodegradable are of scientific and industrial interest due to their biocompatibility and notable performance improvement [1]. Therefore, a large number of research studies dealing with composite materials based on renewable resources have emerged [2-3]. Renewable resources, e.g. cellulose, chitosan, and starch are known to have potential to be key components of biocomposites. These renewable resources can also be easily composted after their intended use without harming the environment [4-5]. Consequently, the use of bio-based composites provides wide ranging opportunities for developing new applications in packaging, building and household materials, electronic and in the automotive, aerospace, and marine fields [6-7].

Cellulose is a natural polysaccharide and one of the most abundant renewable resources on earth. The structure of cellulose consists of a highly crystalline polymer of D-anhydroglucopyranose units joined together in long chains by β-1,4-glycosidic bonds [8]. For many years, cellulose has been a subject of intense study from both of fundamental and practical points of view. Nowadays it has known a modified of this polysaccharide namely regenerated cellulose which is a class of materials manufactured by the conversion of natural cellulose to a soluble cellulosic derivative and subsequent regeneration, typically forming either a fiber or a film. Due to the stiff molecules and close chain packing attributed to strong

* Corresponding author. Tel : +60-85443837
Email address : faisal.amri@curtin.edu.my

DOI: 10.22146/ijc.24310

inter- and intra-molecular hydrogen bonding, cellulose is difficult to dissolve in water and in most common organic solvents [9]. This property is a drawback regarding the processability, fusibility, and functionality of cellulose. Alternatively, ionic liquids have been used as environmentally benign solvents for cellulose dissolution due to their excellent properties such as good chemical and thermal stability, low flammability, low melting point and ease of recycling [10-11]. Currently, a limited number of solvent systems for cellulose have been reported [12-14], and the LiCl/*N,N*-dimethylacetamide (DMAc) system has become very popular due to its advantageous associated with direct dissolution of the cellulose which are being faster, easier and more reproducible [15]. To date, LiCl/DMAc solvent system has also been used as mobile phase in size-exclusion chromatography (SEC) with the column packings such as poly(styrene-divinyl benzene). The solvent and mobile phase being identical simplifies the procedure [16].

It is widely accepted that blending of polymers may the best method of improving the chemical and physical properties of polymer-based composites [17-18]. In a common solvent, polymer blends may form homogeneous solutions. The formation of homogeneous polymer blends can be attributed to strong interaction via hydrogen bonds between the functional groups of the blend components. Cellulose and chitosan are biodegradable and biocompatible polymers; however, they are difficult to process by dissolving into common solvents [19]. This difficulty is mainly due to the presence of intra- and inter-molecular hydrogen bonding and molecular close chain packing. Wu et al. synthesized membranes based on chitosan and cellulose blends using trifluoroacetic acid as a co-solvent [20]. The obtained results indicated that the cellulose/chitosan blends were not well miscible. Stefanescu et al. reported the dissolution of both chitosan and cellulose in 1-butyl-3-methylimidazolium chloride (BMIMCl). They found that high molecular weight chitosan with a Brookfield viscosity of 200,000 cps will only swell in BMIMCl. A complete dissolution of chitosan could not be observed when heating at 100 °C not even after 4 days [21]. In another study, Phisalaphong and co-worker reported the homogenous films of chitosan and bacterial cellulose at concentrations in the range of 0.25–0.75% (w/v) of low molecular weight chitosan [22].

The present work reports a simple method for the preparation of chitosan/regenerated cellulose films with transparent surfaces through the lamination process. It is known that the molecular structures of chitosan and cellulose are very similar, because chemically the only difference between chitosan and cellulose is the presence of fewer $–NH_2$ groups in the former [23]. Therefore, it is expected that both components have high interaction and compatibility with each other. To the best of our knowledge, the study on the formation of biocomposite laminate films from chitosan/regenerated cellulose through dissolution in LiCl/DMAc ionic liquid has not been reported in literature. In this work, chitosan/regenerated cellulose biocomposite laminate films formed by coagulation in water are characterized. The effect of chitosan on the mechanical, morphological and thermal properties of the biocomposite laminate films is discussed.

EXPERIMENTAL SECTION

Materials

The microcrystalline cellulose (MCC) used in this study was a commercial reagent obtained from Sigma Aldrich and had a size of 50 μm. The chitosan (Hunza Nutriceuticals Sdn. Bhd., Malaysia) used had an average size of 80 μm and a 90% degree of deacetylation (DD). The acetic acid (100% v/v), lithium chloride (LiCl) and *N,N,*dimethylacetamide (DMAc) were obtained from Sigma Aldrich.

Procedure

Preparation of the biocomposite laminate films

The chitosan/regenerated cellulose biocomposite laminate films were prepared according to the following procedure; initially, the MCC powders at 1, 2, 4, and 6% (w/v) were dispersed in an ionic solution LiCl/DMAc with constant stirring for 4 h to make a cellulose solution. Meanwhile, the chitosan solution was prepared by dissolving 2 wt% chitosan in an acetic acid solution. The cellulose solution was poured into Petri disks, and stored in an ambient atmosphere for 24 h, corresponding to the formation of a thick transparent gel. Afterwards, the chitosan solution (ratio 1:1 with respect to cellulose) was poured onto the surface of a cellulose gel, and then immersed immediately in distilled water at room temperature for 12 h to remove the ionic liquid residue. Next, the laminate films were dried in a vacuum oven at 35 °C for 2 h. The final films were optically transparent and had a thickness between 0.5 mm and 1.0 mm. The regenerated cellulose films and the chitosan/regenerated laminate films prepared using 1, 2, 4 and 6 wt% cellulose content were coded as RC-1 and RC/Ch-1, RC-2 and RC/Ch-2, RC-4 and RC/Ch-4, RC-6 and RC/Ch-6, respectively.

Characterizations

The tensile tests were performed according to ASTM D 882-10 on an Instron 5582. A minimum of five

specimens of each composition, ranging from 0.5 to 1.0 mm thick, were cut from the sheets. A cross-head speed of 10 mm/min was used, and the test was performed at 25 ± 3 °C.

Thermogravimetric (TGA) and derivative thermogravimetric (DTG) analyses were performed using a TGA Q500 (Perkin Elmer Instrument). The samples were scanned from 30 to 600 °C at a heating rate of 10 °C/min using a nitrogen flow of 50 mL/min.

The morphology of the tensile fracture surface of the biocomposite films was characterized using a scanning electron microscope (SEM), JEOL model JSM 6260 LE. The fracture ends of the specimens were mounted onto aluminium stubs and sputter coated with palladium to avoid electrostatic charging during examination.

X-ray diffraction measurements were performed using an XRD diffractometer (Rigaku Miniflex II) at a scanning rate of 2°/min using Cu-K_α radiation (λ = 0.15406 nm) at 40 kV and 30 mA. All of the samples were scanned in the region of 2θ from 5 to 30° at scanning rate of 1°/min and a step size of 0.01°. Peak fitting was performed using Magic software with a Gaussian function. The relative crystallinity of the biocomposite films were estimated by using Segal's crystallinity index *CrI*, using the following equation [24]:

$$CrI = (I - I')/I \quad (1)$$

where *I* is the amplitude of the diffraction peak (2θ = 22.5–22.7°) and *I′* is the amplitude of the plot at 2θ = 18°. The latter value (*I′*) is used as an indicator of the intensity of the amorphous cellulose.

Fourier transform infra-red spectroscopy (FTIR) was performed on regenerated cellulose and chitosan/regenerated cellulose films in ATR mode (Perkin Elmer 1600 Series). The FT-IR spectra for the samples were scanned from 650 to 4000 cm^{-1} with a resolution of 4 cm^{-1}.

RESULT AND DISCUSSION

Infrared (IR) Spectra and X-Ray Diffraction Analyses

FTIR spectroscopy was used to examine possible interactions between the chitosan and the RC in the laminate films. Fig. 1 shows the infrared (IR) spectra of the microcrystalline cellulose (MCC), the regenerated cellulose (RC) film and the chitosan/regenerated cellulose (RC/Ch) film. As illustrated in the IR spectrum of the MCC, the main characteristic peaks are at approximately 3325 (O–H stretch), 2900 (C–H stretch), 1635 (C–OH stretch) and 1104 (C–O stretch) [25-26]. The IR spectrum of the RC exhibits an increased absorption band of the hydroxyl group from 3325 to 3341 cm^{-1}, indicating the cause of the increased hydrophilic character of the RC. The outcome of the increased hydrophilicity of the RC is attributed to the cleavage of glycosidic bonds (C–O–C) of the cellulose macromolecule, as confirmed by the disappearance of absorption bands at 1104 cm^{-1}. Moreover, a narrow absorption peak was also observed at 1606 cm^{-1}, which corresponds to stretching vibrations of the C–OH group

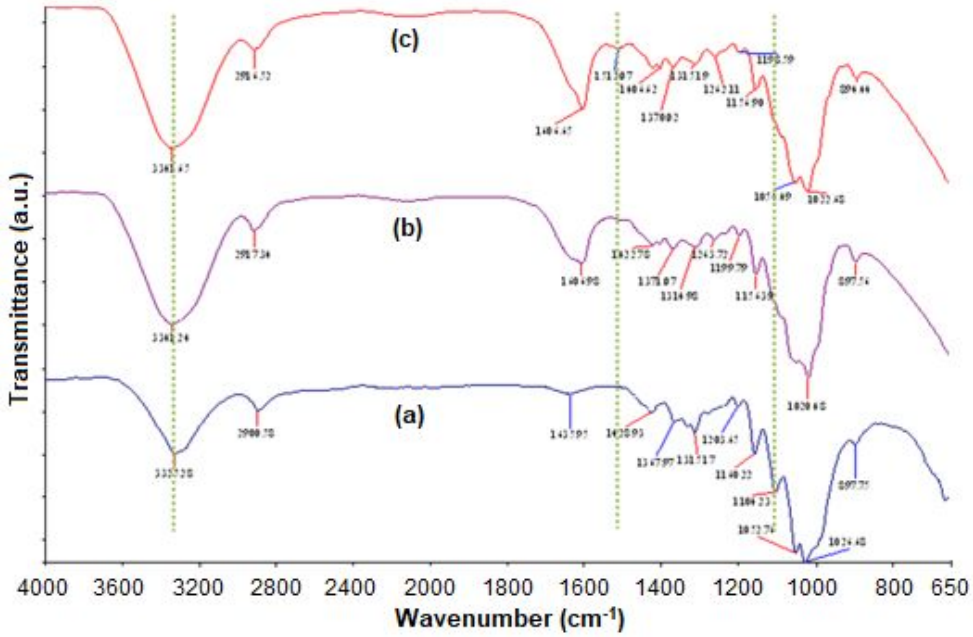

Fig 1. Infrared (IR) spectra of (a) microcrystalline cellulose, (b) RC-4 film and (c) RC/Ch-4 laminate film

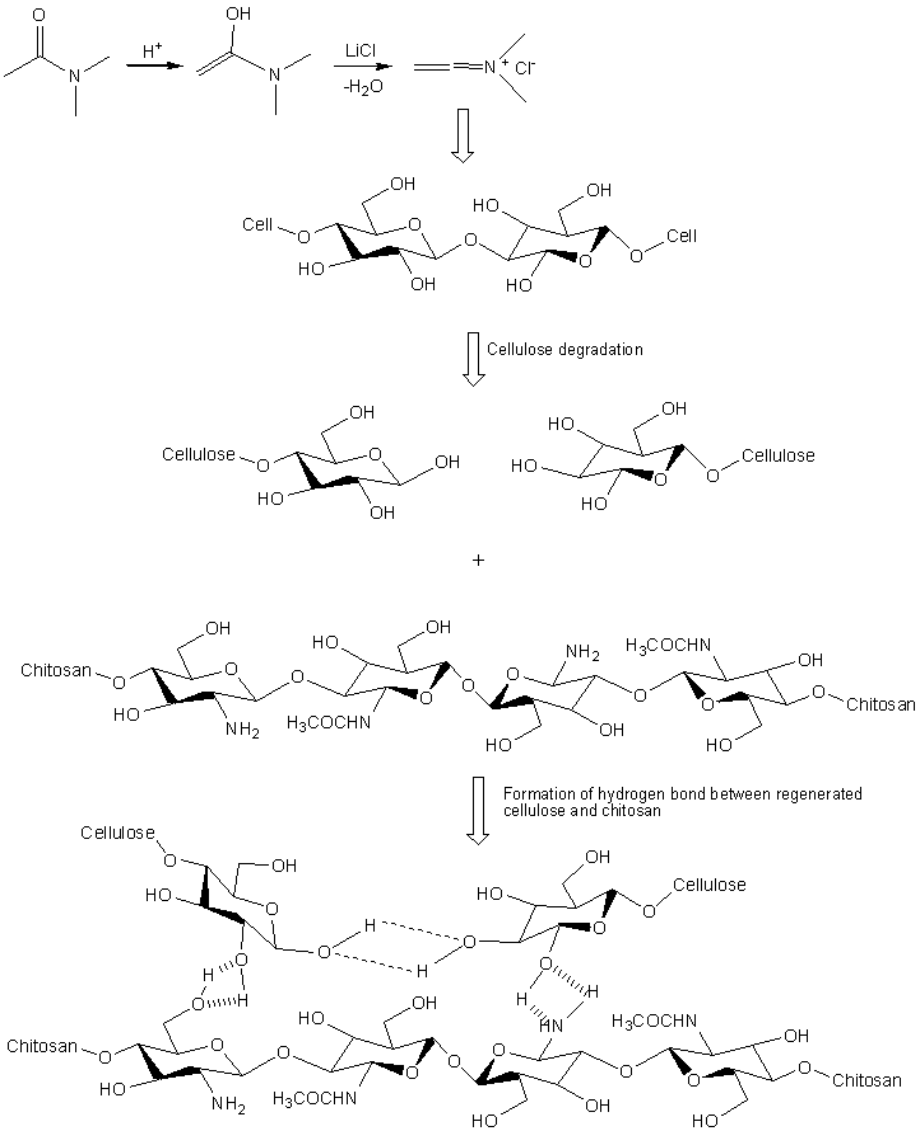

Scheme 1. Proposed schematic degradation of cellulose in LiCl/DMAc ionic liquid and the interaction between chitosan and regenerated cellulose

that is probably due to the increased water content in the solution of cellulose during the regeneration process. Compared to the spectra of the MCC and the RC film, the spectrum of the RC/Ch laminate film is similar to that of the RC film except for the presence of an absorption band at 1512 cm^{-1}. This absorption band corresponds to the N–H bending vibration of the amine group of chitosan. The presence of this band is indicative of the strong interaction via hydrogen bonds between the functional groups of chitosan and the regenerated cellulose leads to the formation of a transparent surface. The proposed schematic of cellulose degradation and the interaction between chitosan and regenerated cellulose is presented in Scheme 1.

Fig. 2 presents the XRD profiles of (a) MCC, (b) RC-4 film, and (c) RC/Ch-4 laminate film, the latter two containing 4 wt% of cellulose content. The MCC exhibited the characteristic peaks to cellulose I at 2θ = 14.98° for the plane, 2θ = 16.6° for the plane and 2θ = 22.7° for the plane. These patterns are typical crystalline domains of this polysaccharide, which are in agreement with the results of previous study [27]. After the regeneration process of the polymer film from the ionic liquid, the regenerated cellulose (RC) films exhibited a diffraction peak at 2θ of 22.5° corresponding to the lattice plane, and no peak appeared at 2θ of 14.9°, which is consistent with a transformation from cellulose I to cellulose II [28]. The *CrI* (0.82) of MCC decreased to 0.48 for RC-4, indicating

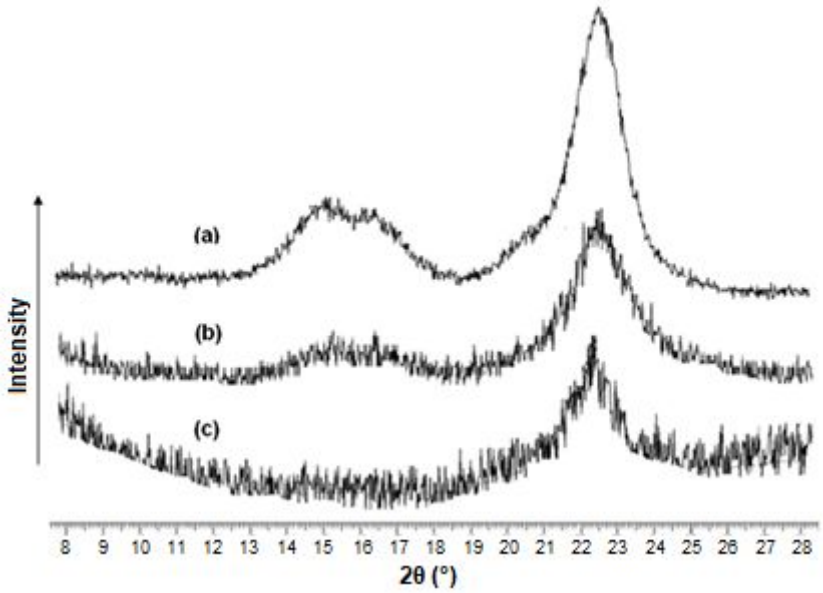

Fig 2. XRD diffraction profiles from (a) microcrystalline cellulose, (b) regenerated cellulose film, and (c) chitosan/regenerated cellulose film. Cellulose content: 4 wt%

Table 1. XRD crystallinity and infrared (IR) crystallinity indexes of RC and RC/Ch laminate films

Sample	X_c (%)	LOI (1428/897)	TCI (1367/2900)
MCC	0.82	0.18	0.98
RC-2	0.61	0.22	0.74
RC-4	0.48	0.25	0.55
RC/Ch-2	0.50	0.19	0.58
RC/Ch-4	0.38	0.23	0.42

that the native crystal structure of cellulose suffers a remarkable decrease in crystallinity as a consequence of dissolving a considerable amount of crystalline cellulose in the ionic liquid. In addition, the observation of the plane of cellulose II contributed to the increased hydrophilic character of the film, as confirmed by the IR spectra. This increased hydrophilic character is a result of the formation of the plane of cellulose II due to stacking of the planar glucan chains through hydrophobic interaction, thereby causing the equatorial hydroxyl groups to be exposed on the sheet plane [29]. However, the diffraction pattern of RC/Ch-4 laminate film was observed to have a peak at 2θ of 22.5° for the lattice plane of cellulose II, with a lower intensity than that of the RC film, which was probably due to the presence of a hydrogen bonding interaction between the functional groups of both components. The presence of this low intensity peak for the laminate film indicates that the cellulose structure was affected by the addition of chitosan. As a result, the *CrI* value of the RC/Ch-4 laminate film decreased to 0.38. This outcome was in agreement with the results of Stefanescu et. al. [30], which indicated that the crystalline peaks of the regenerated cellulose were suppressed upon the addition of chitosan, thereby leading to a significantly lower proportion of crystalline material. In addition, the combination of the two polymers caused the resulting materials to be more amorphous, which explains the disappearance of the sharp diffraction peaks.

In order to better understand the crystallization in the laminate biocomposites, FT-IR was also used to analyse the crystallinity of the biocomposites. This method was initially proposed by Nelson and O'Connor [31], where the crystallinity of the biocomposites was determined by the spectral ratios of 1430/894 and 1374/2923 cm^{-1}. Table 1 presents the XRD crystallinity and the infrared crystallinity for the MCC, the RC films and the RC/Ch laminate films. The obtained results showed that the 1428/897 cm^{-1} ratio (lateral order index, LOI) increased with a decrease of the degree of crystallinity, meanwhile, the 1367/2900 cm^{-1} ratio (total crystalline index, TCI) decreased, indicating that the biocomposites are mainly composed of cellulose II crystal plane. The RC/Ch biocomposites appeared to have lower crystallinity degree as compared with the RC films. The RC/Ch-4 biocomposite film had LOI and TCI index of 0.23 and 0.42, which were remarkably lower than the RC-4 film. A similar result was also found on the results of XRD crystallinity. The FTIR crystallinity results were in agreement with the XRD results.

Tensile Properties of the Biocomposite Laminate Films

A tensile test was conducted to determine the strength of the RC films and the RC/Ch laminate films

when the force is given as tension. Fig. 3 shows the typical stress *versus* strain curves of the RC-2 film, the RC-4 film and the RC/Ch-4 laminate film. Table 2 summarizes the tensile strength, the elongation at break and the Young's modulus of the RC films and the RC/Ch laminate films. As shown in Fig. 3, all the curves exhibited a similar character; however, the RC-4 film exhibited a higher ultimate strength compared to that of the RC-2 film. Furthermore, the presence of chitosan was found to significantly influence the strength of the RC films. Upon the addition of chitosan to the surface of the RC film, the tensile strength decreased, thereby increasing the strain at failure. This outcome revealed that chitosan can greatly enhance the flexibility of the RC films, because cellulose and chitosan have good affinity to each other and mutually augment the resulting properties of the composite films.

As shown in Table 2, the tensile strength and Young's modulus of the biocomposite films improved obviously with the increase of the cellulose content, reaching their maxima at 4 wt%. This improvement is possibly because at a cellulose content of 4 wt%, the number of fibres that are dissolved to form a matrix phase is adequate to provide sufficient intermolecular interaction among the cellulose molecules during the regeneration process. The tensile strength and Young's modulus of RC-4 were 20.57 MPa and 1.02 GPa, respectively. These values for RC-4 were 43.64% and 52.23% higher compared to the tensile strength and Young's modulus of RC-1, respectively, but the value of the elongation at break for RC-4 was lower by 25.62% compared to the RC-1. However, the presence of chitosan also has a detrimental effect on the tensile strength and Young's modulus of RC films. The presence of chitosan influenced the strength of the RC films, resulting in increased ductility. The elongations at break of the RC/Ch biocomposite laminate films increased on average by 61.08% compared to that of the RC films. It is believed that the increased ductility of the RC/Ch laminate films is due to the formation of a hydrogen–bond structure as a consequence of the presence of the high content of hydroxyl functional groups as confirmed by the FTIR analysis.

Scanning Electron Microscope (SEM) Analysis

Fig. 4a, b and c shows SEM micrographs of the tensile fractured surface of the RC-2 film, the RC-4 film and the RC/Ch-4 laminate film, respectively. The micrograph of the RC-2 film (Fig. 4a) appears to exhibit a rough surface with a fibrous-like structure. This fibrous-like structure of the RC biocomposite films is probably attributed to the formation of a nano-fibrillar network between the cellulose molecules during the coagulation process with water. With the addition of a higher cellulose content, the fibrous structure which likely became smaller, led to the formation relative smooth surface and rigid appearance (Fig. 4b), which could be ascribed to the strong interaction between the cellulose molecules. Meanwhile, the micrograph of RC/Ch-4 (Fig. 4c) shows a fracture surface with the appearance of a disorganized structure, which demonstrates the deformability behavior of the biocomposite laminate films with the presence of chitosan. The presence of chitosan clearly changes the surface morphology of the RC films from a rigid to a ductile morphology, corresponding to a decreased

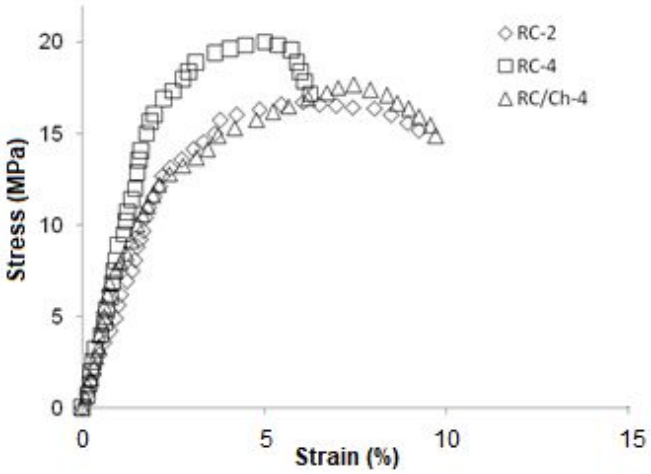

Fig 3. Stress vs. strain data for regenerated cellulose and chitosan/regenerated cellulose at different cellulose content

Table 2. Mechanical properties of RC and RC/Ch laminate films

Sample	Tensile strength (MPa)	Elongation at break (%)	Young's modulus (GPa)
RC-1	14.32 ± 0.86	6.57 ± 0.77	0.67 ± 0.57
RC-2	16.71 ± 0.64	6.22 ± 0.88	0.81 ± 0.51
RC-4	20.57 ± 1.20	5.23 ± 1.05	1.02 ± 0.22
RC-6	18.22 ± 0.75	3.43 ± 0.33	0.83 ± 0.62
RC/Ch-1	10.21 ± 0.50	9.12 ± 0.20	0.53 ± 0.33
RC/Ch-2	12.37 ± 1.32	8.72 ± 1.03	0.62 ± 0.78
RC/Ch-4	17.64 ± 0.87	8.17 ± 0.35	0.77 ± 0.24
RC/Ch-6	15.44 ± 0.98	7.28 ± 0.67	0.69 ± 0.72

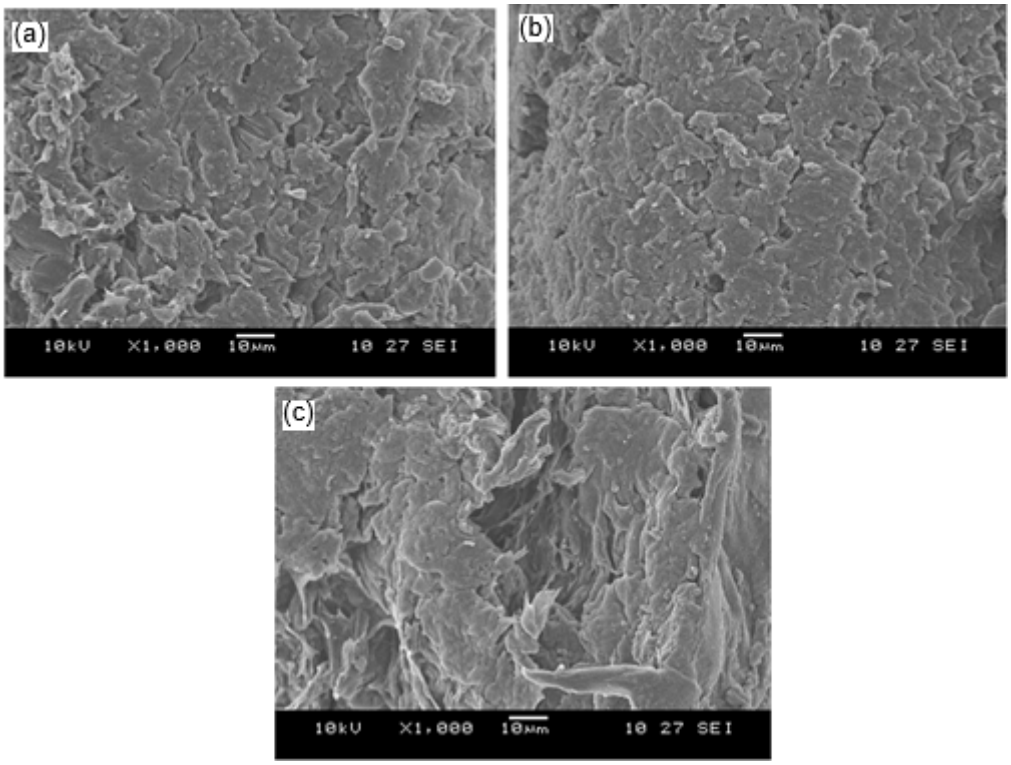

Fig 4. SEM images of fractured surface of (a) regenerated cellulose film with 2 wt% cellulose content, (b) regenerated cellulose film with 4 wt% cellulose content, and (c) chitosan/regenerated cellulose laminate film with cellulose content of 4 wt%

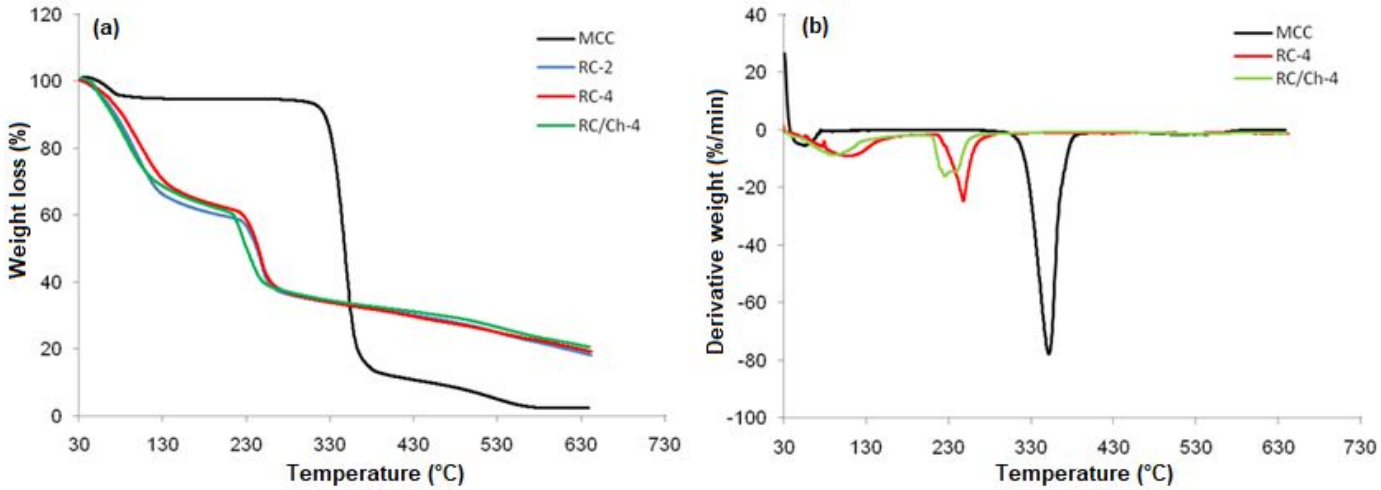

Fig 5. Effect of cellulose content on thermogravimetric properties of regenerated cellulose film and chitosan/regenerated cellulose laminate film. (a) weight loss *versus* temperature curve, (b) derivative thermogravimetric (DTG) curves

degree of crystallinity. This observation apparently indicates that chitosan and regenerated cellulose have formed hydrogen bonds between the functional groups of the two components, leading to the formation of transparent laminate films with ductile behavior.

Thermal Properties of the Biocomposite Laminate Films

Fig. 5a-b shows the TGA and DTG curves of the MCC, the RC films and the RC/Ch laminate films. The higher temperature dramatically increased the weight

Table 3. Percentage of weight loss of MCC, RC-2, RC-4 and RC/Ch-4 biocomposite films at different temperature.

Temperature (°C)	MCC	RC-2	RC-4	RC/Ch-4
50 – 100	4.897	19.678	14.795	20.475
100 – 150	0.441	14.095	15.315	10.291
150 – 200	0.014	3.692	4.366	4.445
200 – 250	0.060	16.341	17.669	21.616
250 – 300	0.742	8.403	9.403	4.081
300 – 350	50.404	2.056	2.456	2.179
350 – 400	31.300	1.804	1.952	1.616
400 – 450	2.257	2.030	2.374	1.648
450 – 500	2.672	2.376	2.168	2.089
500 – 550	3.655	3.324	2.666	3.132
550 – 600	1.210	2.874	2.352	2.727
Total	97.652	76.673	75.516	74.299

loss of all three sample categories, and the results are summarized in Table 3. The thermal degradation of all samples occurred over two-stages: 1) from 50 to 100 °C corresponding to the release of typical strong hydrogen-bonded water; and 2) from 200 to 400 °C, which is associated with decomposition and depolymerization of the cellulose molecules and chitosan polymer. This finding clearly indicates that neither the regeneration process nor the presence of chitosan altered the thermal degradation mechanism of the biocomposite films. In addition, there was another degradation stage occurring from 400 to 600 °C that was attributable to the decomposition of the char residue formed from the second stage.

The curves clearly indicate that the MCC powder has better thermal stability than the RC films and the RC/Ch laminate films, suggesting to positive contribution of the crystalline structure of cellulose I. The regeneration process has obviously changed the molecular structure of cellulose I, yielding the cellulose II structure which is more susceptible to thermal decomposition. As a consequence, the thermal stability of the RC films is lower than that of the MCC. However, the incorporation of the cellulose at a higher content is found to increase the thermal stability of the RC films, probably due to the formation of a sufficient cellulose nano-fibrillar network which efficiently suppresses the heat transfer and leads to the decreased weight losses. The presence of chitosan has shifted the thermal stability of the RC films to a lower temperature, indicating that certain interactions were established between the chitosan and the cellulose.

CONCLUSION

Chitosan/regenerated cellulose laminate films were successfully prepared in LiCl/DMAc ionic liquid. The obtained results revealed the appearance of an absorption band at 1512 cm^{-1} in the IR spectra after the lamination process with chitosan, indicating N–H bending vibrations of the amine group of chitosan on the surface of the regenerated cellulose. The XRD profiles exhibited the formation of a cellulose II lattice plane with a lower intensity than the regenerated cellulose film, indicating a decreased *CrI* value. In addition, the tensile strength was found to decrease with the addition of chitosan at a similar cellulose content; meanwhile, the ductility was increased, as confirmed by the SEM images. This behavior might be due to the formation of hydrogen bonding occurring between the functional groups of the two components, leading to the formation of transparent laminate films with ductile behavior. The TGA study also revealed that the thermal stability of the RC/Ch laminate films shifted to lower temperature.

ACKNOWLEDGEMENT

Research funding from the fundamental research grant scheme (FRGS) by the Ministry of Science and Technology (MOSTI) of Malaysia is greatly acknowledged.

REFERENCES

[1] Vila, C., Campos, A.R., Cristovão, C., Cunha, A.M., Santos, V., and Parajó, J.C., 2008, Sustainable biocomposites based on autohydrolysis of lignocellulosic substrates, *Compos. Sci. Technol.*, 68 (3-4), 944–952.

[2] Panthapulakkal, S., and Sain, M., 2007, Agro-residue reinforced high-density polyethylene composites: Fiber characterization and analysis of composite properties, *Composites Part A*, 38 (6), 1445–1454.

[3] Ibrahim, M.M., Dufresne, A., El-Zawawy, W.K., and Agblevor, F.A., 2010, Banana fibers and microfibrils as lignocellulosic reinforcements in polymer composites, *Carbohydr. Polym.*, 81 (4), 811–819.

[4] Ashori, A., and Nourbakhsh, A., 2009, Characteristics of wood–fiber plastic composites made of recycled materials, *Waste Manage.*, 29 (4), 1291–1295.

[5] Amri, F., Huseinsyah, S., and Hussin, K., 2013, Mechanical, morphological and thermal properties of chitosan filled polypropylene composites: The effect of binary modifying agents, *Composites Part A*, 46, 89–95.

[6] Choi, N.W., Mori, I., and Ohama, Y., 2006, Development of rice husks–plastics composites for

building materials, *Waste Manage.*, 26 (2), 189–194.
[7] Bhattacharyya, D., and Jayaraman, K., 2003, Manufacturing and evaluation of woodfibre-waste plastic composite sheets, *Polym. Polym. Compos.*, 11 (6), 433–440.
[8] Gindl, W., and Keckes, J., 2005, All-cellulose nanocomposite, *Polymer*, 46 (23), 10221–10225.
[9] Bredereck, K., and Hermanutz, F., 2005, Man-made cellulosics, *Rev. Prog. Color. Relat. Top.*, 35 (1), 59–75.
[10] Olivier-Bourbigou, H., Magna, L., and Morvan, D., 2009, Ionic liquids and catalysis: Recent progress from knowledge to applications, *Appl. Catal., A*, 373 (1-2), 1–56.
[11] Rogers, R.D., and Seddon, K.R., 2003, Ionic liquids - solvents of the future?, *Science*, 302 (5646), 792–793.
[12] Mahmoudian, S., Wahit, M.U., Ismail, A.F., and Yussuf, A.A., 2012, Preparation of regenerated cellulose/montmorillonite nanocomposite films via ionic liquids, *Carbohydr. Polym.*, 88 (4), 1251–1257.
[13] Sescousse, R., Gavillon, R., and Budtova, T., 2011, Aerocellulose from cellulose–ionic liquid solutions: Preparation, properties and comparison with cellulose–NaOH and cellulose–NMMO routes, *Carbohydr. Polym.*, 83 (4), 1766–1774.
[14] Han, D., and Yan, L., 2010, Preparation of all-cellulose composite by selective dissolving of cellulose surface in PEG/NaOH aqueous solution, *Carbohydr. Polym.*, 79 (3), 614–619.
[15] Zhang, X., Liu, X., Zheng, W., and Zhu, J., 2012, Regenerated cellulose/graphene nanocomposite films prepared in DMAC/LiCl solution, *Carbohydrate Polym.,* 88, 26-30.
[16] Dupont, A.L., 2003, Cellulose in lithium chloride/*N,N*-dimethylacetamide, optimisation of a dissolution method using paper substrates and stability of the solutions, *Polymer*, 44 (15), 4117–4126.
[17] Zhao, Q., Yam, R.C.M., Zhang, B., Yang, Y., Cheng, X., and Li, R.K.Y., 2009, Novel all-cellulose ecocomposites prepared in ionic liquids, *Cellulose*, 16 (2), 217–226.
[18] Yin, J., Luo, K., Chen, X., and Khutoryanskiy, V.V., 2006, Miscibility studies of the blends of chitosan with some cellulose ethers, *Carbohydr. Polym.*, 63 (2), 238–244.
[19] Almeida, E.V.R., Frollini, E., Castellan, A., and Coma, V., 2010, Chitosan, sisal cellulose, and biocomposite chitosan/sisal cellulose films prepared from thiourea/NaOH aqueous solution, *Carbohydr. Polym.*, 80 (3), 655–664.
[20] Wu, Y.B., Yu, S.H., Mi, F.L., Wu, C.W., Shyu, S.S., Peng, C.K., and Chao, A.C., 2004, Preparation and characterization on mechanical and antibacterial properties of chitsoan/cellulose blends, *Carbohydr. Polym.*, 57 (4), 435–440.
[21] Stefanescu, C., Daly, W.H., and Negulescu, I.I., 2009, Nucleophilic reactivity of chitosan in ionic liquids promoted by tert-amines, *Polym. Prepr.*, 50, 551–552.
[22] Phisalaphong, M., and Jatupaiboon, N., 2008, Biosynthesis and characterization of bacteria cellulose–chitosan film, *Carbohydr. Polym.*, 74 (3), 482–488.
[23] Tran, C.D., Duri, S., Delneri, A., and Franko, M., 2013, Chitosan-cellulose composite materials: preparation, characterization and application for removal of microcystin, *J. Hazard. Mater.*, 252-253, 355–366.
[24] Segal, L., Creely, J.J., Martin, A.E.J., and Conrad, C.M., 1959, An empirical method for estimating the degree of crystallinity of native cellulose using the X-ray diffractometer, *Text. Res. J.*, 29 (10), 786–794.
[25] Liu, Z., Wang, H., Li, Z., Lu, X., Zhang, X., Zhang, S., and Zhou, K., 2011, Characterization of the regenerated cellulose films in ionic liquids and rheological properties of the solutions, *Mater. Chem. Phys.*, 128 (1-2), 220–227.
[26] Da Róz, A.L., Leite, F.L., Pereiro, L.V., Nascente, P.A.P., Zucolotto, V., Oliveira Jr., O.N., and Carvalho, A.J.F., 2010, Adsorption of chitosan on spin-coated cellulose films, *Carbohydr. Polym.*, 80 (1), 65–70.
[27] Ford, E.N.J., Mendon, S.K., Thames, S.F., and Rawlins, J.W., 2010, X-ray diffraction of cotton treated with neutralized vegetable oil-based macromolecular crosslinkers, *J. Eng. Fibers Fabr.*, 5 (1), 10–20.
[28] Ma, H., Zhou, B., Li, H.S., Li, Y.Q., and Ou, S.Y. 2011, Green composite films composed of nanocrystalline cellulose and a cellulose matrix regenerated from functionalized ionic liquid solution, *Carbohydr. Polym.*, 84 (1), 383–389.
[29] Isobe, N., Kim, U.J., Kimura, S., Wada, M., and Kuga, S., 2011, Internal surface polarity of regenerated cellulose gel depends on the species used as coagulant, *J. Colloid Interface Sci.*, 359 (1), 194–201.
[30] Stefanescu, C., Daly W.H., and Negulescu I.I., 2012, Biocomposite films prepared from ionic liquid solutions of chitosan and cellulose, *Carbohydr. Polym.*, 87 (1), 435–443.
[31] Nelson, M.L., and O'Connor, R.T., 1964, Relation of certain infrared bands to cellulose crystallinity and crystal lattice type. Part II. A new infrared ratio for estimation of crystallinity in celluloses I and II, *J. Appl. Polym. Sci.*, 8 (3), 1311–1324.